うな不随意運動の場合，多数の筋からの同時記録を行い，最も早く筋収縮が記録される筋，筋収縮の上行・下行の様式から起源を推測することができる．後述する心因性不随意運動が疑われる場合は表面筋電図を記録しながら，姿勢との関係，出現する状況の特殊性，緊張・精神的負荷などを客観的に評価する必要がある．

2．脳波と表面筋電図の同時記録（脳波・筋電図ポリグラフ）

大脳皮質起源が推測される不随意運動の場合は表面筋電図とともに脳波も同時記録することが必要である．Creutzfeldt-Jakob病（CJD）では自発性ミオクローヌスと脳波上のperiodic synchronous discharge（PSD）と同期する場合がある．

3．誘発筋電図

末梢神経の電気刺激によって誘発される反射性筋放電は短潜時反射（H反射，筋伸張反射）と長潜時反射long-loop reflex（脊髄球脊髄反射spino-bulbo-spinal reflex，皮質経由反射transcortical reflex）に分けられる．皮質反射性ミオクローヌスでは長潜時反射は病的に増強し，C反射と呼ばれる反応が記録される．振戦に対するリセット効果をみる方法もある．振戦が生じている筋を支配する神経に対して超最大電気刺激を与えると誘発筋収縮の後の不応期に続いて振戦の周期がリセットされるが，この不応期がパーキンソン病（約200ms）と本態性振戦（100－120ms）で異なる．

4．Jerk-locked back averaging（JLA）

脳波と不随意運動に伴う筋電図を同時記録し，筋放電の立ち上がりをトリガーとして逆行性に脳波を加算平均することにより，不随意運動に先行する脳活動を記録する方法である[2]．通常の脳波・筋電図ポリグラフでは不随意運動の筋放電に伴って脳波上突発性異常が認められない場合でもこの方法で異常な脳電位が証明されることがある．皮質性ミオクローヌスでは手の不随意筋放電と対側の中心部とくに手の領域に約10～25ms先行して高振幅の脳電位を記録することができる．これは運動皮質の異常興奮を示しており，皮質性と診断できる．一方皮質下性ミオクローヌスではこのような先行脳電位は記録されない．

5．体性感覚誘発電位 somatosensory evoked potential（SEP）

皮質反射性ミオクローヌスの多くはC反射の出現に先行してSEPの皮質成分が非常に巨大（振幅10μV以上）となっている．また2連発電気刺激を与え，刺激間間隔を変えていくと巨大SEPの直後の感覚皮質興奮性の変化（SEP回復曲線）を検討できる[3]．

6．経頭蓋的磁気刺激 transcranial magnetic stimulation（TMS）

不随意運動では運動野の興奮性・抑制性が変化していることが多い．興奮性はMEP閾値が指標となる．ミオクローヌスでは低下していることが多く，抗てんかん薬の服用で高くなる．Cortical silent period（CSP）は抑制系機能の指標となる．二連発磁気刺激法を用いて運動野をいろいろな刺激間間隔でMEP閾値以下の条件刺激とMEP閾値上の試験刺激を与えると1～5msで抑制効果が認められる．詳細は後述する．

心因性不随意運動や陰性現象を見逃さない

心因性と疑われる不随意運動を呈する患者の診断は難しいことが多い[4]．以下の特徴から鑑別する．①突然出現し，突然消失することが多い．②振幅，周波数，分布が変動しやすい．③診察時や観察中は増悪し，誰もいなくなると緩解する．④placeboやsuggestionで増悪あるいは緩解する．⑤注意をそらすと著減する．その際はかなり集中しないとできないような複雑な課題を与えるのが効果的である．⑥心理的背景（抑うつ，疾病利得など）が存在する．また不随意運動は筋収縮だけでなく，筋収縮が維持できない陰性現象のことも

あり，ミオクローヌスやジストニアなどでしばしば観察される．診断に迷ったらビデオ撮影や表面筋電図での確認を繰り返す．

不随意運動を発生源から考える

1．大脳皮質を主な起源とするもの

すべての運動の最終共通路は一次運動野から発するが，その異常興奮によって勝手に筋が収縮する代表的なものがミオクローヌスである．ミオクローヌスは突然生じる瞬間的で jerky な不随意運動であり，短い筋収縮によって生じる陽性ミオクローヌスと持続的筋収縮が突然消失する陰性ミオクローヌスに分けられる．発生起源からは主に皮質性，皮質下性，脊髄性の３つに分類される．さらに網様体性，propriospinal myoclonus も追加される．そのなかで最も多いものが大脳皮質を起源とする皮質性ミオクローヌスである．皮質性はさらに自発性（刺激と無関係に生じる），皮質反射性（刺激過敏性があり，体性感覚，聴覚，視覚刺激などで誘発される），持続性部分てんかん発作 epilepsia partalis continua（EPC）に分けられる．表１にミオクローヌスの主な電気生理学的検査法を示すが多くは皮質性ミオクローヌスの診断に重要なものである．propriospinal myoclonus などの診断には多数筋からの表面筋電図が必要である（図１）[5]．またミオクローヌスでも律動性に生じるものがある．皮質下性（CJD で PSD に関係したもの，アルツハイマー病の一部），脊髄性，皮質性（大脳皮質基底核変性症でのクローヌス様のもの，familial cortical myoclonic tremor with epilepsy での振戦様のもの）などである．Mirror movements も皮質性起源に含まれ，脳梁を介した抑制機能の異常に錐体交叉の異常が加わり複雑なパターンを示す．

表１　ミオクローヌス診断に必要な電気生理学的検査法

- 表面筋電図（拮抗筋が同期，どの筋から始まるか）
- Giant SEP（10μV 以上）
- Jerk-locked back averaging 法（JLA 法）による先行棘波
- Long-loop reflex の亢進（C 反射）
- 磁気刺激（運動閾値の低下）
- SEP 回復曲線

2．基底核運動ループを主な起源とするもの

基底核運動ループは一次運動野，大脳皮質運動関連領野と主に被殻を結ぶもので運動の遂行に関係し[6]，下記の３つの基底核神経回路で調節されている．ハイパー直接路は大脳皮質から興奮性入力を受けた視床下核ニューロン出力核の GABA 作動性ニューロンに単シナプス性に最も短時間に投射する経路である．これによりまず視床－大脳皮質投射ニューロンが広く抑制される．直接路は GABA とサブスタンス P を持つ線条体ニューロンが出力核に単シナプス性に投射する経路で基底核出力を減少させ（脱抑制）随意運動に必要な標的ニューロンが活動する．最後に働くのが間接路であり，GABA とエンケファリンを持つ線条体ニューロンが多シナプス性に淡蒼球外節の GABA 作動性ニューロンと視床下核のグルタミン作動性ニューロンを介して主力核に投射し，標的ニューロンの活動は再び抑制される．このように大脳皮質の状態やそこで取り得る運動を報酬予測に基づいて評価し，それによって運動系列や行動様式を選択している．さらに図２に示すように基底核には意図した運動以外の競合する運動を抑制する働き（周辺抑制：surround inhibition）があり，時間的空間的に運動をコントロールしている[7]．基底核運動ループの異常あるいは周辺抑制の異常によって下記に示すさまざまな不随意運動が生じる．

1）ジストニア

ジストニアとは筋の持続のやや長い収縮で生じるものでジストニア姿勢とジストニア運動からなる．前者は異常収縮の結果としての異常姿勢・異常姿位で，後者は異常収縮によるゆっくりした運動であり，これらはその症例にとって定型的であり，動作特異性や常同性，感覚トリックという特徴を有する．表面筋電図では特定の動作で主動筋と拮抗筋が持続性に共収縮するが動作によってはバースト状に相反性に収縮することもある．ジストニアの発生機序は運動サブルーチン（特定の動

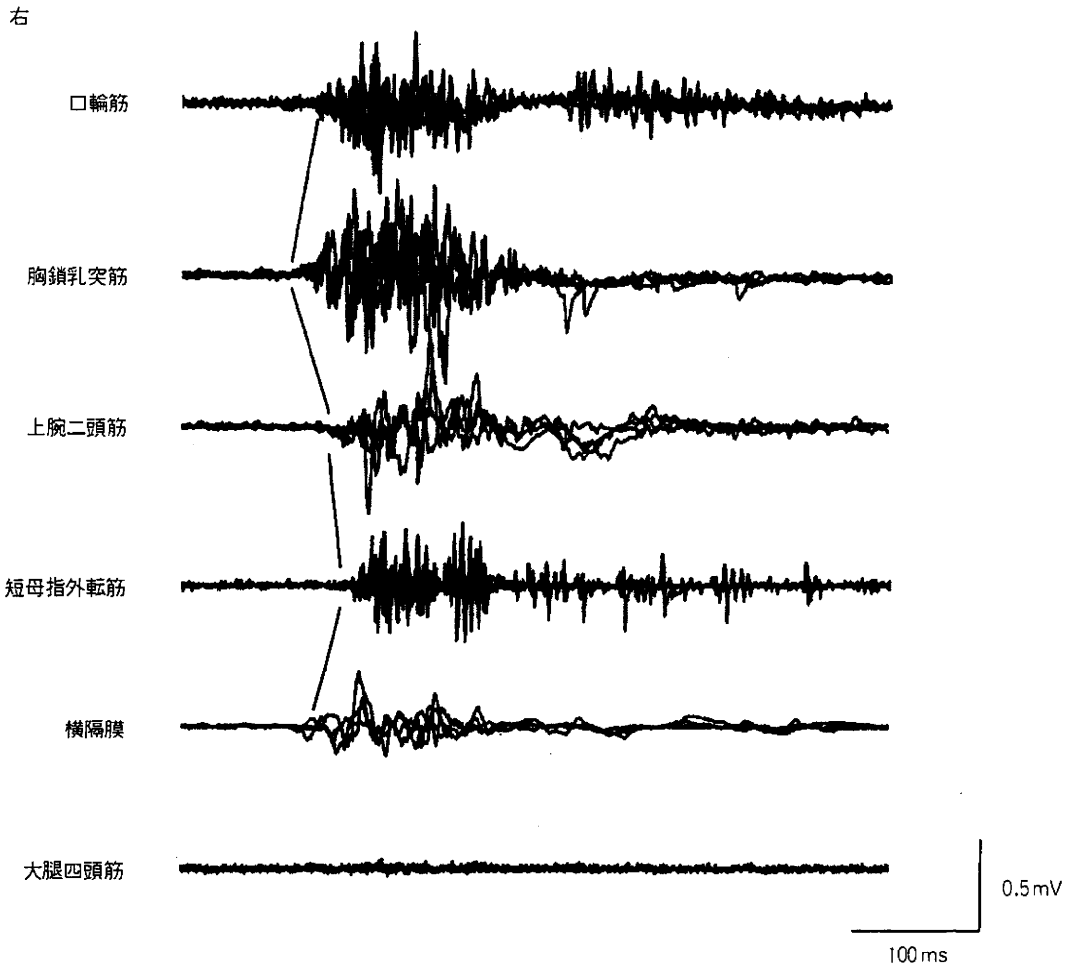

図1　propriospinal myoclonus における表面筋電図
胸鎖乳突筋から始まり，上下に進展することがわかる．

作を繰り返す場合，その動作に必要な固有知覚入力を基に大脳皮質と基底核の間に形成された一定の運動出力）の異常と考えられている．ドーパミンの相対的・絶対的過剰からみると直接路（D1）の過興奮および間接路（D2）の異常による淡蒼球外節の過興奮，視床下核の抑制の結果，淡蒼球内節からの抑制性出力が抑制（脱抑制）されジストニアが生じると考えられている．その結果として運動出力の亢進による個々の筋活動の増加と周辺抑制の低下によって目的に焦点が絞れた運動ができず，競合する筋まで収縮が生じてしまうことになる[8]．周辺抑制機能の評価にはH波やTMSが用いられている．主動筋は運動開始前約100 msから発火まで興奮性が増大し，拮抗筋には相反性抑制がかかっている．図3に示すように正常者では運動準備段階での主動筋（短母指外転筋）のMEP増大と拮抗筋（第一背側骨間筋）のMEP抑制が認められるがジストニア患者では拮抗筋の抑制が障害されている．またMEP変動も正常者では刺激毎に潜時・振幅ともかなり変動するがジストニア患者ではほとんど変動しない（図4）．

2）アテトーゼ

アテトーゼは主として四肢遠位部に絶えず繰り返しみられる緩徐な筋緊張の変動により回転性のよじるような動きである．主動筋と拮抗筋は同期して収縮し，共同運動が困難で各筋がゆっくり勝手に動くので一定の姿勢を保持できない．原因疾患としては脳性麻痺が最も多い．表面筋電図では1～3秒持続する自発的な非律動性群化放電が主動筋と拮抗筋に同期して記録される．

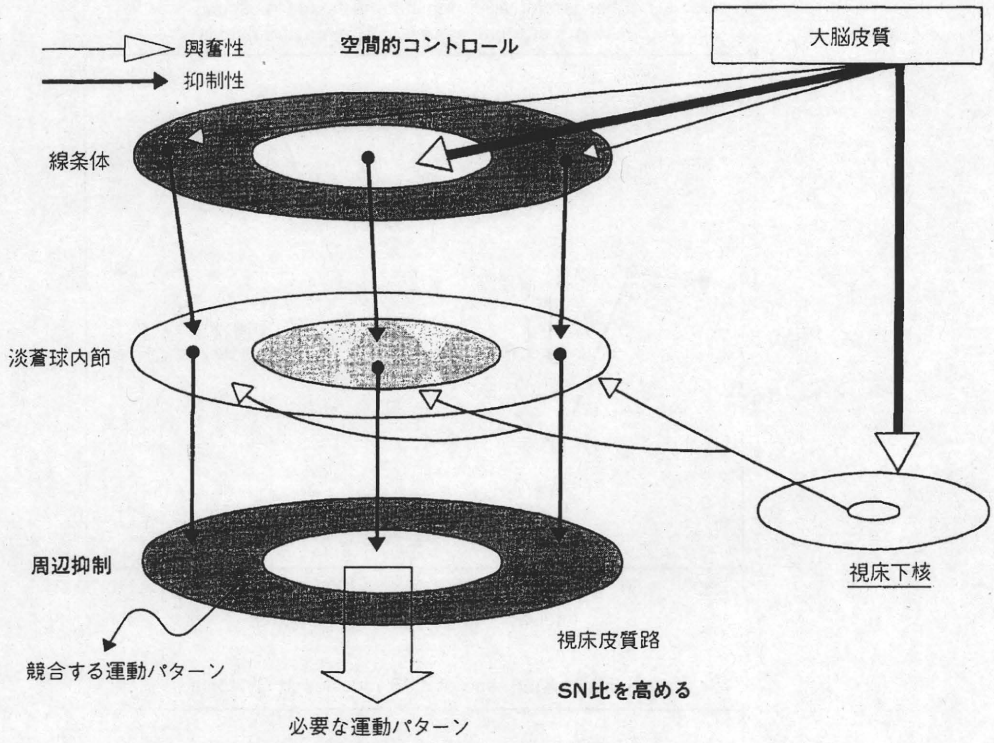

図2　周辺抑制の機能
(Mink JW:2004[7] を改変)

3）舞踏症（舞踏運動）

舞踏症は比較的速く，出現間隔も大きさもまったく不規則な，顔面，四肢，体幹に及ぶ全身性の不随意運動である．精神的緊張や随意運動で増強することが多い．眉をしかめたり，首をすくめたり，手指を進展・屈曲させたりといった落ち着きがない状態と受け止められやすい．表面筋電図では50～300ms位の持続を持つバースト状の筋放電が間隔も大きさも不規則にいろいろな筋に出現する．舞踏症の発生機序としては間接路の異常と考えられており，線条体から淡蒼球外節への抑制がとれることにより，視床下核への抑制が増強し，淡蒼球内節への興奮性作用が低下するために，淡蒼球内節からの抑制性出力が低下し，随意運動を妨げる運動や不要な運動を抑制できなくなるために運動過多となる．

4）バリスム

バリスムは上肢あるいは下肢を投げ出すような激しい動きで片側性のことが多い（片側バリスム）．回旋性要素を伴い，同じパターンの動きを繰り返すが，律動性はない．バリスムは主に視床下核を中心とした間接路が選択的に障害されることにより，視床への抑制がとれて出現する．血管障害や高血糖が原因として多い．被殻淡蒼球病変の関与も推測されている．

3．運動のフィードバック回路を主な起源とするもの

振戦は不随意運動で最も頻度が多いものであるがその発生機序はまだ十分解明されていない．運動をうまく調節するためには主に3つのフィードバック回路が関与していると考えられており，その障害が振戦の発生に関係していることが推測されている[9]．末梢要因として単シナプス性脊髄反射（筋伸長反射）があげられる．中枢要因としては小脳ループと基底核運動ループがあげられる．前者は，大脳皮質－橋核－対側の小脳半球－歯状核－上小脳脚交叉－同側の視床－大脳皮質を中心とした経路である．これらのフィードバックの時間差によって生じた異常振動と中枢での神経細胞

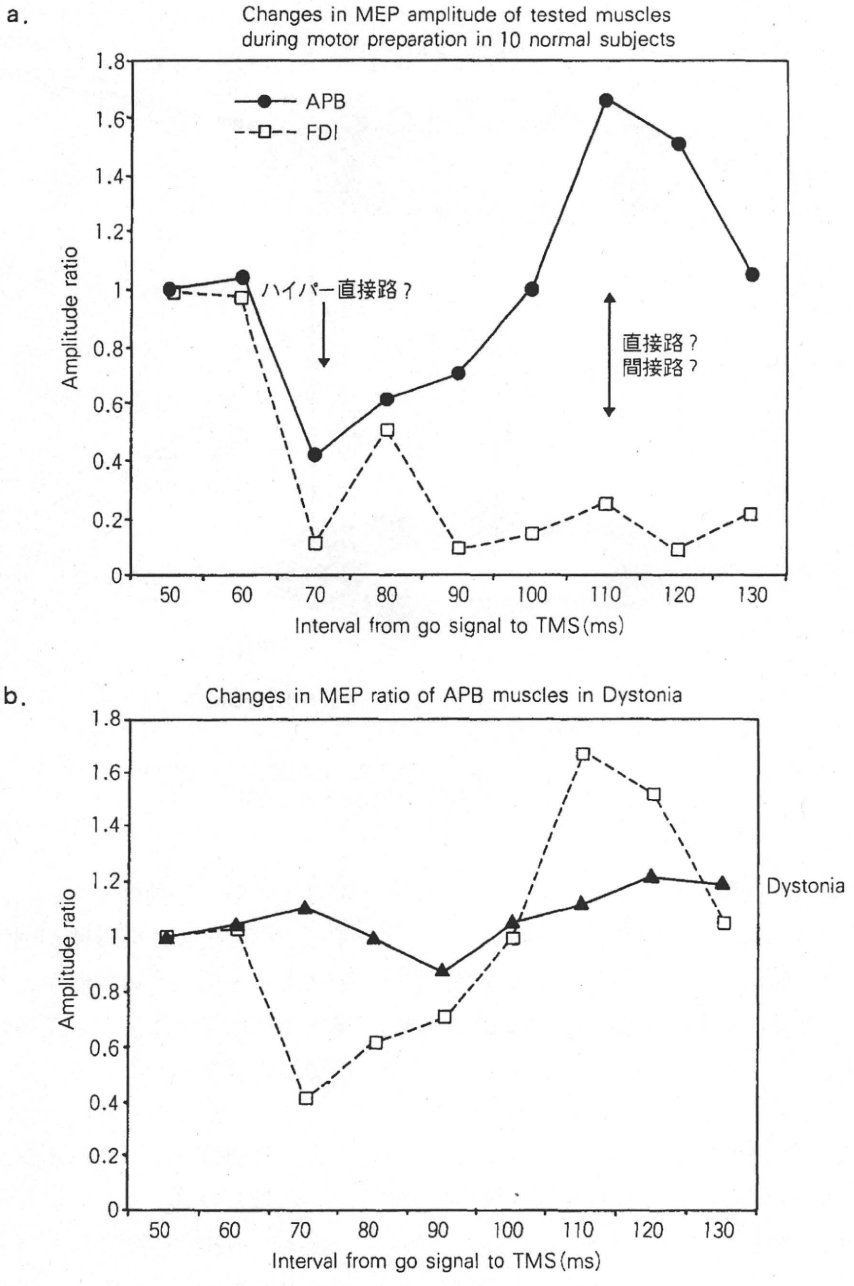

図 3
a：正常者での運動準備段階での主動筋（短母指外転筋）のMEP増大と拮抗筋（第一背側骨間筋）のMEP抑制.
b：ジストニア患者での拮抗筋抑制の障害.

固有の周波数を有する振動（下オリーブ核，視床など）が主な振戦源となる．原則としてフィードバック回路が長ければ振戦の周波数は低くなるし，神経細胞固有の振動に起因した振戦は感覚入力の影響を受けにくい．Parkinson病における安静時振戦は3～6Hzの安静時振戦が片側の上肢から始まることが多い．この振戦の発生には基底核運動ループと小脳ループが相互に関与していることが推測されているがとくに淡蒼球内節と視床下核が重要視されている．

本態性振戦は最も頻度が多い不随意運動であり，両手および両前腕の姿勢時または運動時振戦が主体で，頭部，舌の振戦がみられることがある．周波数は4～12HzでParkinson病の振戦より高い．本

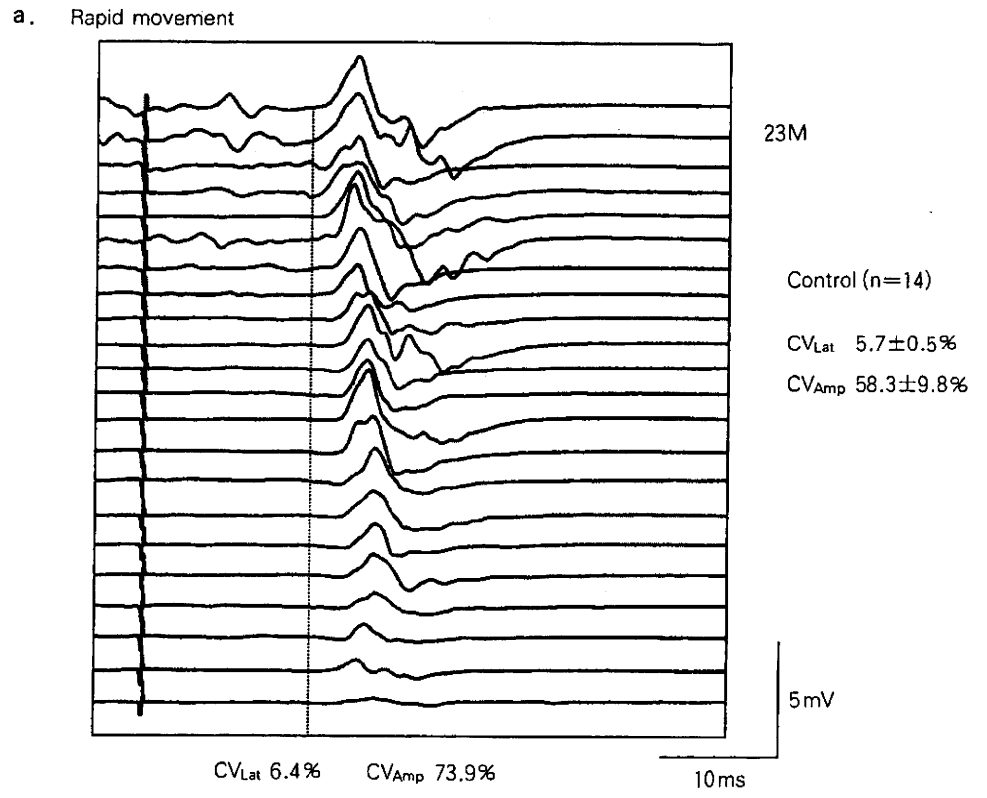

図 4

a：正常者での MEP 変動.

b：ジストニア患者における MEP 変動の著減.

態性振戦の発生起源は未だ確立していないが，末梢起源説よりも中枢起源説（とくに下オリーブ核－小脳系あるいは大脳感覚運動野）が有力である．

動作時振戦・企図振戦は運動の開始直後から始まり，動作が終わると消失する振戦が動作時振戦である．指鼻試験では鼻に到達すると揺れは止まる．

企図振戦は動作に伴って生じる3～6Hzの振戦であり，目的に向かうに従って増強し，かつその姿勢を保つ間も振戦が持続する．いずれも小脳遠心路（上小脳脚を経由する）の障害と考えられている．Holmes振戦（中脳振戦）は安静時および動作時に生じる3Hz程度のゆっくりとした振戦である．Guillain-Mollaret三角（歯状核－対側の赤核－下オリーブ核）の障害とくに赤核周辺の障害から数週から数ヵ月経過して新たな神経結合が生じた結果振戦が生じると考えられている．口蓋振戦は2～3Hzの軟口蓋の振戦であり，喉頭・横隔膜にも生じることがあり，Guillain-Mollaret三角の障害で生じる．

不随意運動を脳のリズムから考える

脳は莫大な数のニューロンが結合した結合振動子系であるという．随意運動に関連してもいくつかの振動ネットワークが存在する．たとえば運動の直前と遂行中に対側の感覚運動野に40～50Hz gamma帯域のevent-related synchronization（ERS）が生じる．また運動終了1～2秒後には15～25Hz beta帯域のERSが認められる．それらの異常が一部の不随意運動の発症にかかわっていると考えられる．また，てんかん患者でも発作開始時にvery fast oscillations（80～500Hz）が認められることがある．4～7Hz oscillationは広い神経ネットワークにかかわり，$GABA_A$抑制に関係すること，15～25Hzはidlingあるいは運動準備状態に関係すること，40～50Hzは局所の神経活動に関与すると考えられている．とくに皮質性ミオクローヌスではあるリズムで皮質興奮性が変動していており[10]，そのリズムを確認するために有用な検査法としてpaired-pulse TMSとjerk-locked MEPがある．

1．15～25Hz oscillation

皮質反射性ミオクローヌスでは二重ときには三重にC反射が誘発されることがある．これらの多重C反射間の潜時差はほとんど40～50msである．JLA法を用いて，C反射に先行する脳波の変化を記録するとC反射と同じリズムで律動性脳波活動が記録される．さらに自発性ミオクローヌスあるいはC反射をトリガーにして刺激間隔を変えながら手の運動野をMEP閾値下の強度で磁気刺激する（jerk-locked MEP）とあるタイミングで磁気刺激した場合にMEPが容易に記録され，このタイミングでは運動野の興奮性が亢進していることが推測され，このときのミオクローヌスあるいはC反射とMEPの潜時差は40～50msである．下肢のみに皮質性ミオクローヌスを呈した1例においてEEG-EMGポリグラフで下肢筋の律動性ミオクローヌスに対応して中心部頭皮上からそれと同じリズムの20～25Hz律動性脳波活動が記録された（図5）．上肢筋と同様にJLA法においてミオクローヌスの前後での律動性脳波活動が下肢の一次運動野付近の頭皮上から記録された．paired-pulse TMSでは刺激間隔45～40msでMEPが容易に刺激された．このように皮質反射性ミオクローヌスを呈した症例の多くで15～25Hzのoscillationが認められ，beta ERSとの関連性が推測される[11]．

2．40～50Hz oscillation

動作性ミオクローヌスを呈した患者では40～50Hz oscillationを示すことが多い．低酸素脳症後に動作性ミオクローヌスを生じた1例を検討するとすばやくボタンを押す動作をさせた場合は約50Hzのリズムを有する筋放電パターンを示し，EEG-EMGポリグラフにおいても筋活動に先行して同じリズムの律動性脳波が記録された．JLA法を用いた検査ではミオクローヌス筋放電に約30ms先行して対側の中心部に脳波上棘波が認められた．paired-pulse TMSでも同様のリズムの

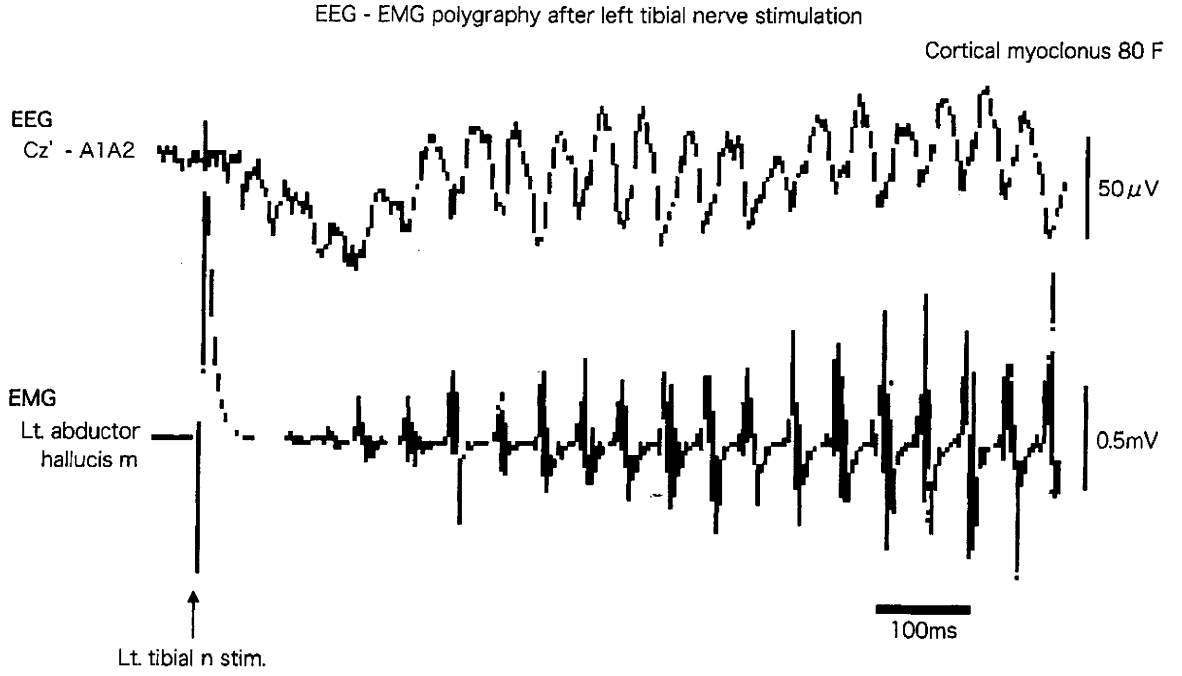

図5　律動性皮質性ミオクローヌス患者で認められた20Hz oscillation

興奮性の変化が証明された[12]．このような動作性ミオクローヌスでは動作時に40～50Hzのoscillationが認められ，随意運動時に観察されるgamma ERSとの関連が推測される．

3．very fast oscillation（80～500Hz）

運動系においても他の大脳皮質と同様にvery fast oscillationが存在することが推測されるがそれを示す十分な証拠は乏しい．C反射は通常はsimpleな波形を示すが時に多相性となる場合がある．各ピークの間隔は2.5～4ms（250～400Hz）であり，very fast oscillationが亢進している可能性が考えられた[13]．また，TMS後に錐体路ニューロンに生じるmultiple I wavesも周期性放電であり，その発射頻度は約500～700Hzである．これが体性感覚野や視覚野で認められるhigh frequency oscillations（HFOs）と同じ機序あるいは意義を持つのか不明である．しかし，ある種のてんかんでvery fast oscillationの亢進が観察され，ミオクローヌス患者で感覚野のHFOsが高振幅であることが報告されており[14]，皮質興奮性の異常を生じる点では共通点がある．

4．大脳皮質基底核変性症（CBD）におけるoscillation

CBDにおけるミオクローヌスは他の疾患で認められるミオクローヌスと比べて以下に示すような異なった特徴を有する．①運動拙劣を示す上肢に目立つ，②安静時よりも動作時に顕著となり，特に指を押すなどの負荷を与えて筋緊張を高めることで誘発されやすく，その場合は一見律動性で（6～7Hz）クローヌス様に見える，③giant SEPは認められず，むしろ皮質反応は低振幅のことが多い，④JLA法でもpremyoclonic spikeが認められない，⑤C反射は記録されるがその潜時差から計算されるcortical delay timeは短く，感覚野経由した反射とは考えにくい，⑥40～50Hzのoscillationが認められることが多い．EEG-EMGポリグラフにおいて約40Hzの律動性活動が記録された症例での自発性ミオクローヌスをトリガーとしたjerk-locked MEPではC反射と23msの間隔でMEPが誘発される刺激タイミングにおいて皮質興奮性が亢進していることが示された．

不随意運動を神経ネットワークから考える

M1の出力に影響を与える大脳皮質領域は多数存在するが，とくに運動前野（PMd，PMv）補足運動野，頭頂葉後部（PPC），感覚野が重要である．また小脳からの影響も重要である．これらのネットワーク機能をみる方法としてその領域にTMSあるいはrTMSを条件刺激として与え，MEPへの影響をみることが行われている[15]．

1．運動前野刺激

同側のPMdに対して閾値下の単発TMSあるいは1 Hz rTMSを与えるとMEPは振幅低下し，5 Hz rTMSでは振幅増大する．これらの方法を用いてジストニアでのPMd-M1抑制性結合低下が証明されている[16]．さらには二重条件刺激の影響や対側のPMdからの影響も検討されている．

2．小脳刺激

小脳にTMSを与えることにより大脳皮質運動野へのTMSあるいは電気刺激により導出されるMEPが抑制され，小脳失調患者では異常となることが報告されている[17]．小脳条件刺激のためにはダブルコーンコイルの中心を後頭孔隆起上と外耳孔を結ぶ線上を後頭孔隆起より3 cm外側の部位に置き，コントロール波形に比べて，刺激間隔5 msで抑制が始まり，3～4 ms抑制が持続する．この効果は小脳刺激によって小脳皮質のプルキンエ細胞が刺激され，歯状核にインパルスが伝わり，小脳－視床－大脳皮質回路が賦活化され，皮質運動野を抑制することが推測されている

上腕二頭筋を随意収縮した状態でダブルコーンコイルを用いて小脳外側部にTMSを加えると同側の上腕二頭筋から潜時約26～28msで促通効果が生じ，それに続いて約50ms持続する抑制効果が認められる．右視床出血後6ヵ月経過した頃から左上肢の協調運動障害に加えて約3 Hzの動作時振戦を認めた患者で小脳核視床路の障害が推測されたが，この方法での左上腕二頭筋での反応が消失していた[18]．

薬理学的に不随意運動を考えてみる

TMSを用いた運動野の興奮性をみる検査法は表2に示すように多数開発されている．しかもそ

表 2

a：運動野興奮性をみるためのMEP測定法

Single TMS
Motor threshold (MT)
MEP amplitude (MEP)
Cortical silent period (CSP)
Paired TMS
Short-interval intracortical inhibition (SICI)：1－5 ms
Intracortical facilitation (ICF)：7－20ms
Short-interval intracortical facilitation (SICF)：約1.5ms毎
Long-interval intracortical inhibition (LICI)：50－200ms
末梢神経刺激
Short latency afferent inhibition (SAI)：2－8 ms

b：TMSと薬理学的意義

MT：Na^+channel阻害剤で低下
MEP：$GABA_AR$ agonistsで低下，SSRIで上昇など
CSP：$GABA_AR$を反映．強刺激で$GABA^BR$も
SICI：$GABA_AR$を反映
ICF：GABA? glutamate?
SICF：興奮性介在ニューロン（I wave産生）
LICI：$GABA_BR$を反映
SAI：cholinergic function?

の薬理学的意義もかなり解明されており，これらの方法を用いてそれらの薬理学的異常がヒトでも検討できるようになってきた[19]．とくに不随意運動において研究が進んでおり，ミオクローヌスではshort-interval intracortical inhibition (SICI) の低下とintracortical facilitation (ICF) の亢進，本態性振戦ではICFの亢進，ジストニアではCSPの短縮，SICIの低下およびshort latency afferent inhibition (SAI) の亢進，舞踏様運動ではCSPの短縮，SICIの減弱，long-interval intracortical inhibition (LICI) の亢進およびICFの亢進，チックではSICIの短縮などが報告されている．

おわりに

不随意運動を理解するには，その発生起源や病態を考えて検査法を選択する必要がある．磁気刺激法などの検査法の発展により，病態生理の解明が進むものと期待される．

文　献

1) 魚住武則：不随意運動の診かた（1）臨床脳波 48：533－560, 2006.
2) Shibasaki H, Kuroiwa Y : Electroencephalographic correlates of myoclonus. Electroenceph clin Neurophysiol 39 : 455－462, 1975.
3) Ugawa Y, Genba K, Shimpo T et al : Somatosensory evoked potential recovery (SEP-R) in myoclonic patients. Electroenceph clin Neurophysiol 80 : 21－25, 1991.
4) Brown P, Thompson PD : Electrophysiological aids to the diagnosis of psychogenic jerks, spasms, and tremor. Mov Disord 16 : 595－599, 2001.
5) Brown P, Pothwell JC, Thompson PD et al : Propriospinal myoclonus : Evidence for spinal "pattern" generators in humans. Mov Dis 9 : 571－576, 1994.
6) Alexander GE, Crutcher MD : Functional architecture of basal ganglia circuits : neural substrates of parallel processing. Trends Neurosci 13 : 381－425, 1990.
7) Mink JW : The basal ganglia and involuntary movements : impaired inhibition of competing motor patterns. Arch Neurol 60 : 1365－1368, 2003.
8) Sohn YH, Hallett M : Disturbed surround inhibition in focal hand dystonia. Ann Neurol 56 : 595－599, 2004.
9) Rodger JE : Origins of tremor. The Lancet 355 : 1113－1114, 2000.
10) Ugawa Y, Hanajima R, Terao Y et al : Exaggerated 16-20Hz motor cortical oscillation in patients with positive or negarive myoclonus. Clin Neurophysiol 114 : 1278－1284, 2003.
11) 魚住武則，玉川　聡，辻　貞俊：皮質性ミオクローヌス患者における感覚運動野の律動性活動．臨床脳波 46：791－800, 2004.
12) Uozumi T, Tamagawa A, Hashimoto T et al : Rhythmic EMG and EEG activity during voluntary movement in posthypoxic cortical action myoclonus. J UOEH 27 : 227－236, 2005.
13) Uozumi T, Tamagawa A, Hashimoto T et al : High-frequency oscillations in the human motor system. Clin Neurophysil (Suppl) 59 : 143－147, 2006.
14) Mochizuki H, Ugawa Y, Machii K et al : Somatosensory evoked high-frequency oscillations in Parkinson's disease and myoclonus epilepsy. Clin Neurophysiol 110 : 185－191, 1999.
15) Reis J, Swayne OB, Vandermeeren Y et al : Contribution of transcranial magnetic stimulation to the understanding of cortical mechanisms involved in motor control. J Physiol 586 : 325－351, 2008.
16) Koch G, Schneider S, Baumer T et al : Altered dorsal preotor-motor interhemispheric pathway activity in focal arm dystonia. Mov Disord 23 : 660－668, 2008.
17) Ugawa Y, Terao Y, Hanajima R et al : Magnetic stimulation over the cerebellum in patients with ataxia. Electroenceph clin Neurophysiol 104 : 453－458, 1997.
18) 魚住武則，武智詩子，玉川　聡，ほか：小脳磁気刺激の臨床応用　臨床脳波 48：657－664, 2006.
19) Paulus W, Classen J, Cohen LG et al : State of the art : Pharmacologic effects on cortical excitability measures tested by transcranial magnetic stimulation Brain stim 1 : 151－163, 2008.

110　変形性筋ジストニアの予後，就業

Q 41歳の女性で全身性ジストニア（dystonia musculorum deformans：変形性筋ジストニア）と診断された社員のことでお尋ねします．入社当時は自力歩行可能で徒歩にて通勤していましたが，徐々に四肢，体幹の変形がひどくなり，自力歩行不能になって自家用車で通勤しています．近年は体幹部の変形もひどくなり，力も入りにくくなっているようです．職場周囲からみて自家用車による通勤についても不安があります．いろいろ調べてみましたが，マイナーな疾患で将来的な展開が予測できず，対応に苦慮しています．そこで次のことについて教えてください．

①疾病の予後について：将来的には寝たきりになることも予想されますが，何歳頃にどのようになる可能性がありますか．

②治療による改善の可能性（現在は近隣の病院で内服加療をしています）．

③専門医からみた車両運転や就業可能なレベルの程度について．

④患者会などの有無．

A dystonia musculorum deformans（DMD）とは，一次性捻転ジストニア（primary torsion dystonia）ともよばれる一次性全身性ジストニアを表す言葉です．一般には，遺伝性ジストニアの一つであるDYT1ジストニアとほぼ同義として用いられていますが，他の全身性ジストニアを生じる疾患が混ざってしまう可能性があります．そのため，今日ではDMDのような言葉はあまり用いられなくなり，遺伝子検査で確定したもののみをDYT1ジストニア（あるいはOppenheimジストニア）とよび，その他のものはnon-DYT1として扱われることが多くなっています．

今回のご相談では，DMDという診断名ですので，この名前だけでは二次性ジストニアがどこまで鑑別されているかもわからないため，予後等を判断するのはかなり困難です．

point

・全身性ジストニアは，原因となる疾患の種類により経過や予後は異なる．

・脳深部刺激のような新しい治療法があり，専門外来でのフォローアップが望ましい．

予　後

上述の通り，DMDと診断されうるものの大半はDYT1ジストニアです．典型的なDYT1ジストニアは，学童期に一側の下肢か一側の腕に始まり，他の身体部分に広がります．発症後5～10年の進行が顕著であることが知られており，全身に広がって臥床状態となることも少なくありません．発症年齢によって予後が大きく異なることが知られており，成人発症例では症状が局所にとどまるものもあります．この方の発症時期は記載がありませんのでわかりませんが，41歳になる現在も進行が明らかであるところをみると，DYT1ではないのかもしれません．DYT1ジストニアの平均発症年齢は12歳であり，20歳以上での発症はまれです．non-DYT1の場合は，遺伝性のもののほかにジストニアを生じる他疾患を除外する必要もあり，予後に関しては一概には言えません．症状の進行具合から判断するしかないと思います．

治　療

一般に，ジストニアには内服（抗コリン薬，ハロペリドール，バクロフェン，Lドーパ，ジアゼパムなど），ボツリヌス毒素局所注射，手術（脳深部刺激，定位脳手術）が用いられますが，診断により治療は変わります．もしDYT1遺伝子変異が発見されれば，脳深部刺激（deep brain stimulation：DBS）治療が著効することが知られており，逆にボツリヌス毒素局所注射で増悪することがあります．この理由でDYT1遺伝子は最低でも確認しておきたいところです．DBSは，non-DYT1でも部分的ではありますが効果があります．なお，ボツリヌス毒素は施注した筋のみに効果がありますので，通常は全身性の場合には適応になりません．

運転・就業

ジストニアは持続性の筋収縮を呈する病態です．素早くハンドルを切る，ブレーキを踏むなどの動作は困難になることが予測されます．また，体幹の変形が著しくなると，周囲の確認が困難になるでしょう．坐位での迅速な上肢・下肢の運動が可能かなどの要素を勘案して判断することになると思います．

就業についてですが，病型によっては知能の障害が出てきますので，その要素が入る可能性もあります．DYT1ジストニアでは知能は正常に保たれます．知能が正常であれば頭脳労働・監視業務などは可能であると思われますので，最も問題となるのは通勤かもしれません．

患者会

2005年5月にNPO法人ジストニア友の会が発足しています．活動内容などはホームページ（http://www.geocities.jp/dystonia2005/index.html）を参照してください．まず，診断を遺伝子変異も含めて決定することが重要だと思いますので，ジストニア専門外来を開設している病院にかかってみてはいかがでしょうか．通院中の病院がジストニア専門であれば，DBSなどを含めた治療法について尋ねてみるべきだと思います．

（玉川　聡）

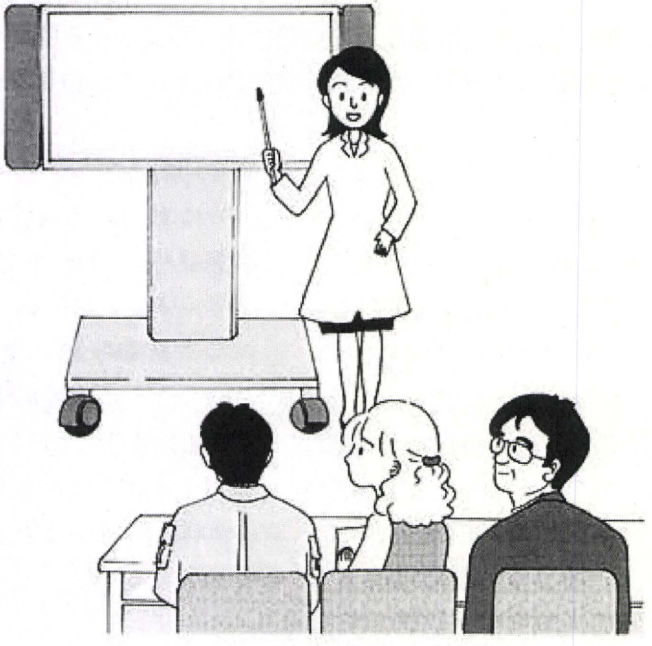

Biochemical and Biophysical Research Communications 391 (2010) 242–247

Contents lists available at ScienceDirect

Biochemical and Biophysical Research Communications

journal homepage: www.elsevier.com/locate/ybbrc

Prevention of intracellular degradation of I2020T mutant LRRK2 restores its protectivity against apoptosis

Etsuro Ohta [a], Makoto Kubo [a], Fumiya Obata [a,b,*]

[a] Division of Clinical Immunology, Graduate School of Medical Sciences, Kitasato University, 1-15-1 Kitasato, Sagamihara, Kanagawa 228-8555, Japan
[b] R & D Center for Cell Design, Institute for Regenerative Medicine and Cell Design, Kitasato University School of Allied Health Sciences, 1-15-1 Kitasato, Sagamihara, Kanagawa 228-8555, Japan

ARTICLE INFO

Article history:
Received 5 November 2009
Available online 11 November 2009

Keywords:
Parkinson's disease
Leucine-rich repeat kinase 2
PARK8
Apoptosis

ABSTRACT

Leucine-rich repeat kinase 2 (*LRRK2*) is the causal gene for autosomal dominant familial Parkinson's disease. We have previously reported a novel molecular feature characteristic to I2020T mutant LRRK2: higher susceptibility to post-translational degradation than the wild-type LRRK2. In the present study, we demonstrated that the protective effect of I2020T LRRK2 against hydrogen peroxide-induced apoptosis was impaired in comparison with the wild-type molecule. When the intracellular level of the protein had been allowed to recover by treatment with proteolysis inhibitors, the protective effect of I2020T LRRK2 against apoptosis was increased. We further confirmed that a decrease in the intracellular protein level of WT LRRK2 by knocking down resulted in a reduction of protectivity against apoptosis. These results suggest that higher susceptibility of I2020T mutant LRRK2 to intracellular degradation than the wild-type molecule may be one of the mechanisms involved in the neurodegeneration associated with this LRRK2 mutation.

Introduction

Parkinson's disease (PD) is a movement disorder caused by degeneration of dopaminergic neurons. *Leucine-rich repeat kinase 2* (*LRRK2*) is the gene responsible for autosomal dominant PD, PARK8, which we originally defined by linkage analysis of a Japanese family (Sagamihara family) [1–4]. LRRK2 belongs to the receptor-interacting protein (RIP) family, which has LRR (leucine-rich repeat), ROC (Ras of complex), COR (C-terminal ROC), kinase, and WD40 domains [5]. The Sagamihara family patients have the I2020T mutation in the kinase domain [4,6]. Up to now, a total of 23 LRRK2 mutations in various domains have been reported worldwide [2–4,7]. Patients with LRRK2 mutations exhibit clinical features indistinguishable from those of patients with sporadic PD, and LRRK2 is postulated to be a key molecule in the etiology of the disease. However, its true physiological function or the mechanism of neurodegeneration resulting from the mutation has not been conclusively clarified.

Accumulated data suggest that hyper-kinase activity reported for mutant LRRK2 molecules, particularly G2019S LRRK2, may be one possible mechanism for the pathogenesis induced by this molecule [8–13]. It has also been postulated that autophosphorylation of LRRK2 stabilize the kinase-active dimer and exacerbates the pathogenesis [14]. In the case of I2020T mutation, however, there is a degree of controversy; some studies have reported augmented kinase activity [9,15,16], whereas other studies of this mutation have demonstrated unchanged or impaired phosphorylation activity [11,17,18]. Thus, at least in the case of I2020T mutation, there is no consensus on the mechanism responsible for neurodegeneration.

In the previous study, we demonstrated that I2020T LRRK2 is more susceptible to post-translational degradation than the wild-type LRRK2 and G2019S LRRK2, indicating a novel molecular feature characteristic to I2020T LRRK2 [19]. In the present study, we investigated whether the high degradation rate of I2020T LRRK2 is related to the pathogenesis associated with this mutant molecule. We found that the wild-type LRRK2 exhibited a protective effect against apoptosis whereas I2020T mutant LRRK2 had impaired protectivity. Prevention of the intracellular degradation of I2020T LRRK2 markedly increased its protective effect against apoptosis. Finally, we investigated the relationship between the intracellular protein level of LRRK2 and its protectivity against apoptosis employing a LRRK2-knockdown experiment.

Materials and methods

Transfection of LRRK2. The mammalian expression cDNA construct of wild-type (WT) and I2020T mutant *LRRK2* cDNA with a V5 tag at the C-terminus was described previously [19]. Sequence

* Corresponding author. Address: Division of Immunology, School of Allied Health Sciences, Kitasato University, 1-15-1 Kitasato, Sagamihara, Kanagawa 228-8555, Japan. Fax: +81 42 778 8075.
E-mail address: obata@ahs.kitasato-u.ac.jp (F. Obata).

0006-291X/$ - see front matter © 2009 Elsevier Inc. All rights reserved.
doi:10.1016/j.bbrc.2009.11.043

analysis proved that T6059>C (I2020T) at exon 41 was the only difference between the WT and the I2020T *LRRK2* cDNA construct throughout the whole plasmid. HEK293 cells were cultured in Dulbecco's modified Eagle medium (DMEM) (Sigma) supplemented with 10% FCS and antibiotics. SH-SY5Y cells were cultured in DMEM nutrient mixture F-12 HAM (Sigma) supplemented with 10% FCS, and antibiotics. Transfection of the *LRRK2* cDNA plasmid was performed using Lipofectamine™ 2000 (Invitrogen) for HEK293 cells, and FuGENE® HD Transfection Reagent (Roche) for SH-SY5Y cells in accordance with the manufacturers' protocols. SH-SY5Y clones stably and uniformly expressing WT or I2020T LRRK2 have been described previously [19].

Western analysis. LRRK2-transfected cells were suspended in cell lysis buffer [Tris–HCl-buffered saline (pH 7.6) containing 1% digitonin, 1 mM phenylmethylsulfonyl fluoride, and 1 tablet of Complete mini protease inhibitor cocktail® (Roche)]. Cell lysates were obtained by centrifugation and subjected to Western analysis using horseradish peroxidase (HRP)-labeled antibody against the V5 tag (Invitrogen) for LRRK2 expression and HRP-labeled antibody against β-actin (Abcam) as an internal control.

Prevention of intracellular degradation of LRRK2. After 24 h of transfection with WT and I2020T *LRRK2* cDNA, HEK293 cells were treated with a cocktail of three proteolysis inhibitors, 1 μM MG-132 (Calbiochem) and 1 μM lactacystin (Sigma), both of which are proteasome inhibitors, and with 200 nM chloroquine (Sigma), a lysosome inhibitor. After 24 h of treatment, the cells were harvested and their lysates were analyzed by Western blotting, as described above. The stably LRRK2-expressing SH-SY5Y clones were also treated with the proteolysis inhibitors for 24 h and analyzed in the same manner.

Hydrogen peroxide (H_2O_2)-induced apoptosis. Apoptosis was induced by treatment of LRRK2-transfected cells with various concentrations (1–6 mM) of H_2O_2 for 50 min at 37 °C. In some experiments, the cells were treated with a cocktail of the proteolysis inhibitors MG-132, lactacystin and chloroquine for 24 h before addition of H_2O_2. Percentage of apoptotic cells was measured using an Annexin V-PE apoptosis Kit I™ (BD Biosciences) and an EPICS XL™ Flow Cytometer (Beckman Coulter) in accordance with the manufacturer's protocol. Apoptotic cells were also assessed by Western analysis of the lysates of transfected cells using an antibody against caspase-9 (Cell Signaling). For cell viability analysis, LRRK2-transfected cells were treated with 0.5 mM H_2O_2 for 30 min at 37 °C, and subjected to assay using a Cell Counting Kit-8™ (Dojindo) in accordance with the manufacturer's protocol.

Knockdown of transfected LRRK2. HEK293 cells were transfected with WT LRRK2 cDNA together with 25mer of Stealth™ RNAi for LRRK2 (5′-GAGCUGCUCCUUUGAAGAUACUAAA-3′; Invitrogen) or with an RNAi-control with the scrambled sequence. The effectiveness of knockdown of transfected LRRK2 was confirmed by Western analysis using anti-V5 antibody. After 24 h of co-transfection, the cells were treated with various concentrations (0.05–3 mM) of H_2O_2 for 30 min to induce apoptosis, and cell viability was analyzed.

Results

H_2O_2-induced apoptosis in LRRK2-transfected cells

To elucidate the physiological function of LRRK2 in the maintenance of cell viability, H_2O_2-induced apoptosis in LRRK2-transfected HEK293 cells was analyzed using annexin V staining. Among WT LRRK2-transfected cells treated with H_2O_2, the percentage of apoptotic cells was significantly lower than among untransfected cells, which expressed only endogenous LRRK2 molecules (Fig. 1A). In contrast, the percentage of apoptotic cells among I2020T mutant LRRK2-transfected HEK293 cells was significantly higher than that among WT LRRK2-transfected cells, and not significantly different

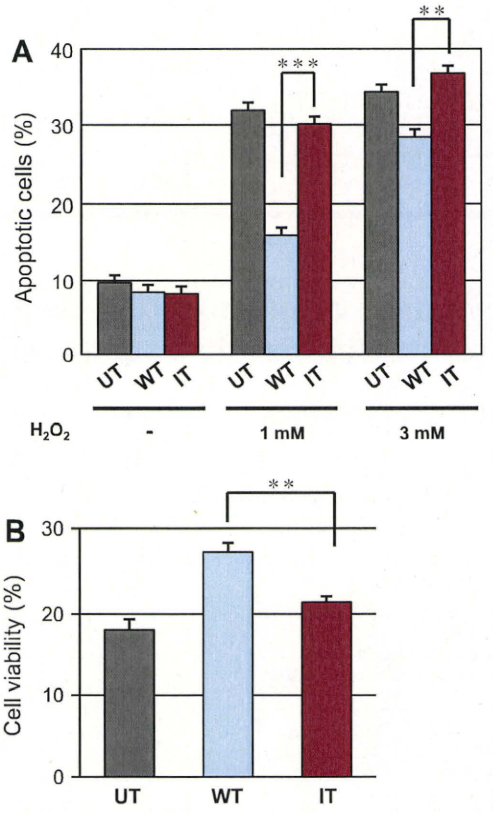

Fig. 1. H_2O_2-induced apoptosis in LRRK2-transfected cells. (A) WT and I2020T (IT) LRRK2-transfected HEK293 cells were treated with 1 or 3 mM H_2O_2 for 50 min. The percentage of cells showing apoptosis was measured by annexin V staining. (B) WT and I2020T (IT) LRRK2-transfected HEK293 cells were treated with 0.5 mM H_2O_2 for 30 min and the cell viability was measured. UT: Untransfected HEK293 cells. Stars represent statistical comparisons by one-way ANOVA ($n = 3$); $^{**}p < 0.005$. $^{***}p < 0.0005$.

from the situation in untransfected cells. Similar results were obtained for the LRRK2-transfected neuroblastoma cell line SH-SY5Y, although to a less marked extent due to the low transfection efficiency, and for SH-SY5Y clones stably and uniformly expressing WT or I2020T LRRK2 (Supplementary Fig. 1A and B). Consistently, the viability of I2020T LRRK2-transfected HEK293 cells was significantly lower than that of the WT LRRK2-transfected cells (Fig. 1B). These results suggest that WT LRRK2, but not I2020T mutant LRRK2, exerts a protective effect against H_2O_2-induced apoptosis.

Apoptosis of LRRK2-transfected cells after treatment with proteolysis inhibitors

In the previous study, we demonstrated that the I2020T mutant LRRK2 is more susceptible to post-translational degradation than the WT LRRK2 [19]. To investigate whether prevention of degradation of the mutant LRRK2 influences its ability to protect against H_2O_2-induced apoptosis, WT- and I2020T LRRK2-transfected HEK293 cells were treated with a cocktail of proteolysis inhibitors, MG-132 (a proteasome inhibitor), lactacystin (a proteasome inhibitor), and chloroquine (a lysosome inhibitor). As reported, treatment with this inhibitor cocktail increased the I2020T LRRK2 protein to a level similar to that of WT LRRK2 (Fig. 2A). Possibly because of the apoptosis-promoting effect of the protease inhibitors [20,21], the treatment significantly increased the percentage of annexin V-positive apoptotic cells among WT LRRK2-transfected cells, although the percentage was still lower than that among

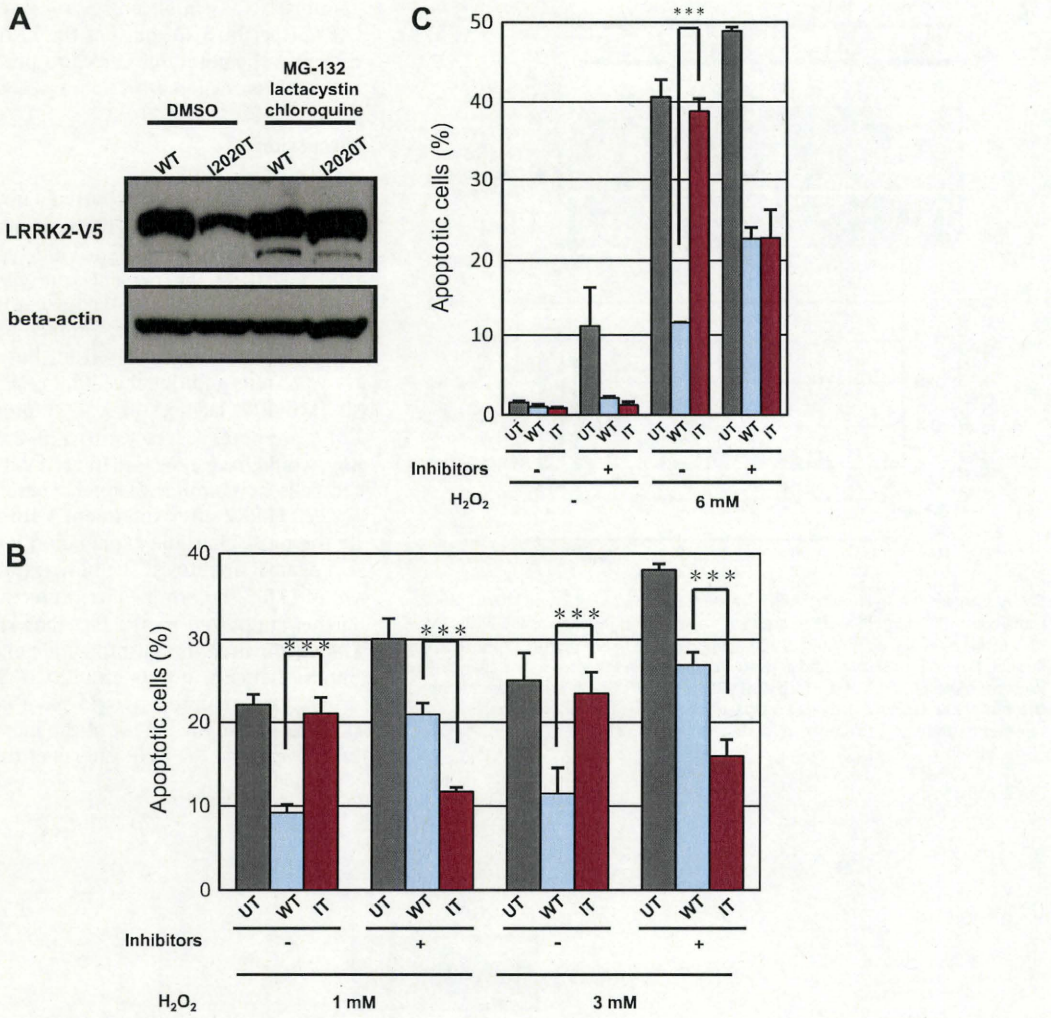

Fig. 2. Effect of proteolysis inhibitors on apoptosis in LRRK2-transfected cells. (A) HEK293 cells were transfected with WT or I2020T LRRK2 cDNA and treated with a cocktail of three proteolysis inhibitors (1 μM MG-132, 1 μM lactacystin, and 200 nM chloroquine) for 24 h. The LRRK2 level in the lysates was then analyzed by Western blotting with an antibody against V5 tag. (B) WT and I2020T (IT) LRRK2-transfected HEK293 cells were treated for 24 h with a cocktail of proteolysis inhibitors, and apoptosis was induced with 1 or 3 mM H_2O_2 for 50 min. UT: Untransfected HEK293 cells. (C) SH-SY5Y clones stably and uniformly expressing WT and I2020T LRRK2 (IT) were treated for 24 h with a cocktail of proteolysis inhibitors, and apoptosis was induced with 6 mM H_2O_2 for 4 h. UT: Untransfected SH-SY5Y cells. The percentage of apoptotic cells was measured by annexin V staining. Stars represent statistical comparisons by one-way ANOVA ($n = 3$); $^{***}p < 0.0005$.

untransfected cells subjected to the same treatment (Fig. 2B). Nevertheless, the same treatment of I2020T LRRK2-transfected cells markedly decreased the percentage of apoptotic cells to a level even lower than that among WT LRRK2-transfected cells.

Next, the effect of proteolysis inhibitors on apoptosis was analyzed using SH-SY5Y clones that over-expressed the WT and I2020T LRRK2 molecules stably and uniformly. Treatment with the proteolysis inhibitors increased the percentage of apoptotic cells among the WT LRRK2-expressing clones, although the percentage was still lower than that among the control cells (Fig. 2C). On the other hand, in I2020T LRRK2-expressing clones, the same treatment, which would otherwise have impaired the ability to protect against apoptosis, dramatically reduced the percentage of apoptotic cells to a level similar to that among the WT LRRK2-expressing clones. These results indicated that the ability of I2020T LRRK2 to protect against apoptosis could be restored by preventing its intracellular degradation.

Apoptosis was also analyzed by activation of caspase-9. The molecular ratio of activated relative to inactive caspase-9 in H_2O_2-treated cells was higher in I2020T LRRK2-transfected HEK293 cells than in WT LRRK2-transfected cells (Fig. 3). Although treatment with the proteolysis inhibitors increased the molecular ratio of activated caspase-9 in both WT- and I2020T LRRK2-transfected cells, this treatment reduced the ratio of activated caspase-9 in the I2020T LRRK2-transfected cells to a level lower than that in the WT LRRK2-transfected cells. These results, in terms of both annexin V staining and caspase-9 activation, indicated that the ability of I2020T LRRK2 to protect cells against apoptosis can be increased by preventing its degradation.

Influence of LRRK2-knockdown on protectivity against apoptosis

Finally, the relationship between the intracellular protein level of LRRK2 and protectivity against apoptosis was investigated in a knockdown experiment. Transfection of *LRRK2*-specific RNAi together with WT *LRRK2* cDNA into HEK293 reduced the protein level of transfected WT LRRK2 to 18% in comparison with the use of an RNAi-control (Fig. 4A). As described above, transfection of WT *LRRK2* cDNA into HEK293 markedly improved the viability of H_2O_2-treated cells (Fig. 4B). This protectivity of WT LRRK2 against

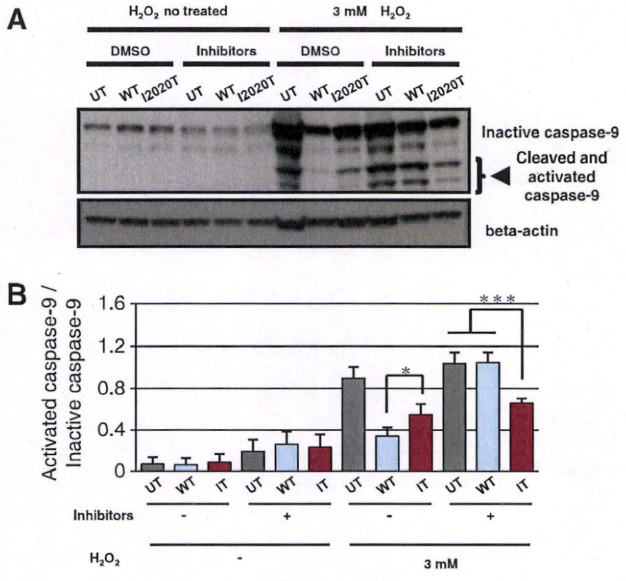

Fig. 3. Caspase-9 activation in LRRK2-transfected cells. (A) WT- and I2020T LRRK2-transfected HEK293 cells were treated with a cocktail of proteolysis inhibitors (MG-132, lactacystin and chloroquine), and apoptosis was induced with 3 mM H_2O_2 for 50 min. The level of cleaved and activated caspase-9 in the lysates was analyzed by Western blotting. UT: Untransfected HEK293 cells. (B) Graphical representation of the molecular ratio of activated caspase-9 relative to inactive caspase-9. Stars represent statistical comparisons by one-way ANOVA ($n = 3$); $^{*}p < 0.05$. $^{***}p < 0.0005$.

apoptosis was significantly abrogated by co-transfection of the LRRK2-specific RNAi but not the RNAi-control. These results indicate that the ability of LRRK2 to protect cells from H_2O_2-induced apoptosis is related with its intracellular protein level.

Discussion

We have previously reported a novel molecular feature characteristic to I2020T LRRK2: that it is more susceptible to post-translational degradation than the wild-type LRRK2 and G2019S mutant LRRK2 [19]. In the present study, we found that the increased intracellular protein level achieved by preventing degradation of I2020T LRRK2 restore its protectivity against apoptosis. Indeed the protease inhibitors used in this study have been reported to show various additional cellular effects, e.g., promotion of apoptosis (MG-132, lactacystin, and chloroquine) and activation of the CMV promoter (lactacystin) [20–25]. However, such effects, if any, would have appeared in both WT- and I2020T LRRK2-transfected cells in a similar manner. Therefore, an increased amount of I2020T LRRK2 after treatment with proteolysis inhibitors would be the most plausible explanation for the increased protective effect against apoptosis. The notion that the intracellular protein level of LRRK2 determines its protective effect against apoptosis is further supported by the fact that knockdown of transfected WT LRRK2 impaired its cell-protective effect. Similarly, the apparently opposite effects in WT- and I2020T LRRK2-transfected cells after proteolysis treatment would have been due to the fact that, in the latter case, the extent of the increased protective effect might have overcome the toxic effects of the inhibitors. When its degra-

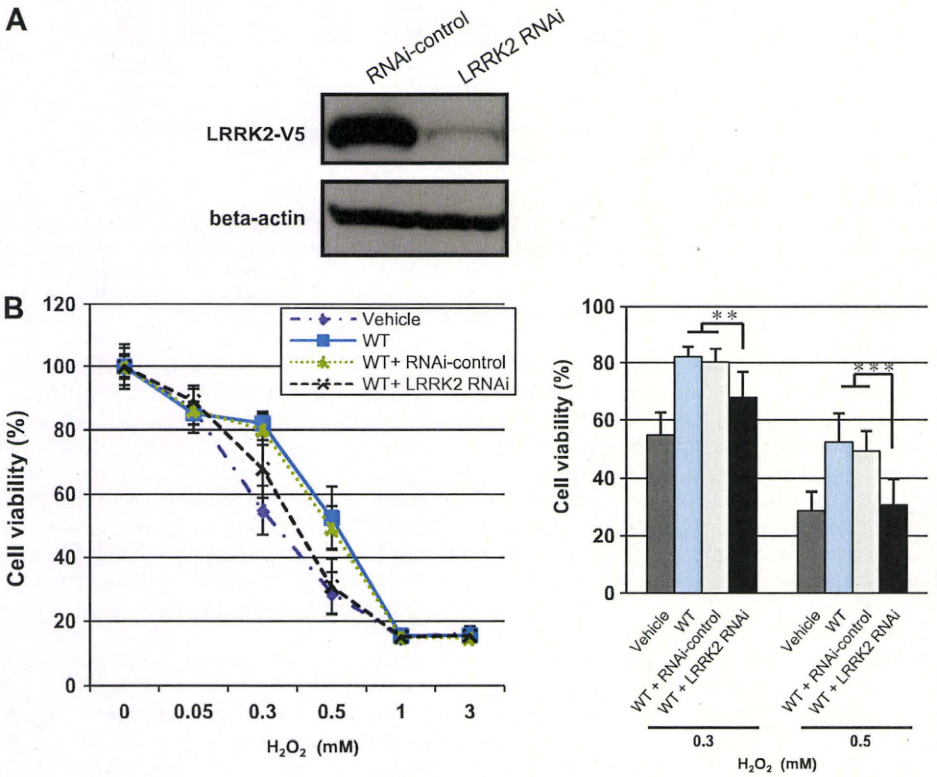

Fig. 4. Effect of a decrease in LRRK2 protein level on protectivity against apoptosis. HEK293 cells were transfected with WT *LRRK2* cDNA together with the LRRK2-specific RNAi or with the RNAi-control having the scrambled sequence. (A) After 24 h of co-transfection, the protein level of transfected WT LRRK2 was analyzed by Western blotting using anti-V5 antibody. (B) The cells after 24 h co-transfection were treated with 0.05, 03, 0.5, 1, or 3 mM H_2O_2 for 30 min to induce apoptosis, and cell viability was measured. Dash-dotted line (–·–·–): vehicle, solid line (—): WT *LRRK2* cDNA, dashed line (– –): WT *LRRK2* + LRRK2 RNAi, dotted line (·····): WT *LRRK2* + RNAi-control. The results of treatment with 0.3 and 0.5 mM H_2O_2 are also represented by bar graph. Stars represent statistical comparisons by one-way ANOVA ($n = 6$); $^{**}p < 0.005$. $^{***}p < 0.0005$.

dation was prevented, the I2020T LRRK2 expressed by HEK293 exhibited an even stronger protective effect against apoptosis, in terms of both annexin V and caspase-9 analysis, than WT LRRK2, suggesting that I2020T LRRK2 might have a higher intrinsic potential than WT LRRK2 to activate a yet unknown apoptosis–protection pathway.

Although in the present study we found that the WT LRRK2 had a protective effect against H_2O_2-induced apoptosis and that knockdown of the WT LRRK2 abrogated this effect, there has been some controversy as to whether LRRK2 is protective or toxic for cells [12,15,26–28]. Under our experimental conditions, we did not observe any increase of apoptosis in WT LRRK2-transfected cells without H_2O_2 treatment. However, we could not exclude the possibility that over-expressed WT LRRK2 exerts a cytotoxic effect on cells in a steady state, whereas it functions as a maintenance or protective molecule when cells are exposed to oxidative stress. Interestingly, loss of the LRRK2-orthologue in *Drosophila* has been reported to induce an increase in susceptibility to oxidative stress and a lower survival rate, being consistent with the results of our LRRK2-knockdown experiments [29].

Although hyper-kinase activity of mutant LRRK2 molecules, particularly G2019S LRRK2, has been reported to be one possible mechanism for the pathogenesis induced by this molecule [8–13,15], there is controversy in the case of I2020T mutation. Some studies have reported augmented kinase activity [9,15,16], whereas other studies of this mutation have demonstrated unchanged or impaired kinase activity [11,17,18]. The results presented here suggest a new neurodegenerative mechanism induced by I2020T LRRK2, i.e., higher susceptibility to degradation gives rise to insufficiency of functional molecules to protect neurons from apoptosis. Several reports have revealed that insufficiency of gene products can cause dominant hereditary neurodegeneration, e.g., progranulin in frontotemporal lobar degeneration linked to chromosome 17 [30], transforming growth factor beta 2 and neurotrophin receptor trkB/C in the mouse PD model [31,32], and p73 in the mouse Alzheimer's disease model [33]. In addition, because LRRK2 has been reported to form dimers [9,34], any postulated molecular instability leading to degradation of I2020T LRRK2 may influence the stability and/or function of not only the I2020T/I2020T-homodimer but also the WT/I2020T-heterodimer, as is the case for GTP cyclohydrolase I in DYT5 dystonia [35,36] and KIT (mast/stem cell growth factor receptor) in piebaldism [37,38]. Finally, as in the case of I2020T LRRK2, the G2019S mutant LRRK2 exhibited impaired protectivity against H_2O_2-induced apoptosis (data not shown). As we reported previously, the G2019S LRRK2 does not differ from WT LRRK2 in susceptibility to degradation [19]. It cannot be excluded that each type of LRRK2 mutation affects a different molecular aspect of LRRK2, i.e., kinase activity, dimer formation, or susceptibility to degradation, all of which finally lead to neurodegeneration through a common and/or an independent pathway.

Conclusion

The intracellular protein level of LRRK2 determines protectivity against H_2O_2-induced apoptosis. The protective effect of I2020T mutant LRRK2 against apoptosis can be restored by preventing its intracellular degradation. Our results suggest a new etiology of neurodegeneration in PD caused by the LRRK2 mutation.

Acknowledgments

This study was supported by the Japanese Ministry of Education and Technology (Grant-in-Aid for Young Scientists, B-21790848), Kitasato University (All Kitasato Project Study, No. 18-1), by a Kitasato University Research Grant for Young Researchers of 2009, and the Graduate School of Medical Sciences, Kitasato University (Integrative Research Program, 2008–2009).

Appendix A. Supplementary data

Supplementary data associated with this article can be found, in the online version, at doi:10.1016/j.bbrc.2009.11.043.

References

[1] M. Funayama, K. Hasegawa, H. Kowa, M. Saito, S. Tsuji, F. Obata, A new locus for Parkinson's disease (PARK8) maps to chromosome 12p11.2–q13.1, Ann. Neurol. 51 (2002) 296–301.
[2] A. Zimprich, S. Biskup, P. Leitner, P. Lichtner, M. Farrer, S. Lincoln, J. Kachergus, M. Hulihan, R.J. Uitti, D.B. Calne, A.J. Stoessl, R.F. Pfeiffer, N. Patenge, I.C. Carbajal, P. Vieregge, F. Asmus, B. Müller-Myhsok, D.W. Dickson, T. Meitinger, T.M. Strom, Z.K. Wszolek, T. Gasser, Mutations in LRRK2 cause autosomal-dominant Parkinsonism with pleomorphic pathology, Neuron 44 (2004) 601–607.
[3] C. Paisan-Ruiz, S. Jain, E.W. Evans, W.P. Gilks, J. Simon, M. van der Brug, A. Lopez de Munain, S. Aparicio, A.M. Gil, N. Khan, J. Johnson, J.R. Martinez, D. Nicholl, I.M. Carrera, A.S. Pena, R. de Silva, A. Lees, J.F. Martí-Massó, J. Pérez-Tur, N.W. Wood, A.B. Singleton, Cloning of the gene containing mutations that cause PARK8-linked Parkinson's disease, Neuron 44 (2004) 595–600.
[4] M. Funayama, K. Hasegawa, E. Ohta, N. Kawashima, M. Komiyama, H. Kowa, S. Tsuji, F. Obata, An LRRK2 mutation as a cause for the Parkinsonism in the original PARK8 family, Ann. Neurol. 57 (2005) 918–921.
[5] E. Meylan, J. Tschopp, The RIP kinases: crucial integrators of cellular stress, Trends Biochem. Sci. 30 (2005) 151–159.
[6] E. Ohta, K. Hasegawa, T. Gasser, F. Obata, Independent occurrence of I2020T mutation in the kinase domain of the leucine rich repeat kinase 2 gene in Japanese and German Parkinson's disease families, Neurosci. Lett. 417 (2007) 21–23.
[7] U. Kumari, E.K. Tan, LRRK2 in Parkinson's disease: genetic and clinical studies from patients, FEBS J., in press.
[8] A.B. West, D.J. Moore, S. Biskup, A. Bugayenko, W.W. Smith, C.A. Ross, V.L. Dawson, T.M. Dawson, Parkinson's disease-associated mutations in leucine-rich repeat kinase 2 augment kinase activity, Proc. Natl. Acad. Sci. USA 102 (2005) 16842–16847.
[9] C.J. Gloeckner, N. Kinkl, A. Schumacher, R.J. Braun, E. O'Neill, T. Meitinger, W. Kolch, H. Prokisch, M. Ueffing, The Parkinson disease causing LRRK2 mutation I2020T is associated with increased kinase activity, Hum. Mol. Genet. 15 (2006) 223–232.
[10] E. Greggio, S. Jain, A. Kingsbury, R. Bandopadhyay, P. Lewis, A. Kaganovich, M.P. van der Brug, A. Beilina, J. Blackinton, K.J. Thomas, R. Ahmad, D.W. Miller, S. Kesavapany, A. Singleton, A. Lees, R.J. Harvey, K. Harvey, M.R. Cookson, Kinase activity is required for the toxic effects of mutant LRRK2/dardarin, Neurobiol. Dis. 23 (2006) 329–341.
[11] B. Luzon-Toro, E.R. de la Torre, A. Delgado, J. Perez-Tur, S. Hilfiker, Mechanistic insight into the dominant mode of the Parkinson's disease-associated G2019S LRRK2 mutation, Hum. Mol. Genet. 16 (2007) 2031–2039.
[12] W.W. Smith, Z. Pei, H. Jiang, V.L. Dawson, T.M. Dawson, C.A. Ross, Kinase activity of mutant LRRK2 mediates neuronal toxicity, Nat. Neurosci. 9 (2006) 1231–1233.
[13] D. Macleod, J. Dowman, R. Hammond, T. Leete, K. Inoue, A. Abeliovich, The familial Parkinsonism gene LRRK2 regulates neurite process morphology, Neuron 52 (2006) 587–593.
[14] S. Sen, P.J. Webber, A.B. West, Leucine-rich repeat kinase 2 (LRRK2) kinase activity: dependence on dimerization, J. Biol. Chem., in press.
[15] A.B. West, D.J. Moore, C. Choi, S.A. Andrabi, X. Li, D. Dikeman, S. Biskup, Z. Zhang, K.L. Lim, V.L. Dawson, T.M. Dawson, Parkinson's disease-associated mutations in LRRK2 link enhanced GTP-binding and kinase activities to neuronal toxicity, Hum. Mol. Genet. 16 (2007) 223–232.
[16] Y. Imai, S. Gehrke, H.Q. Wang, R. Takahashi, K. Hasegawa, E. Oota, B. Lu, Phosphorylation of 4E-BP by LRRK2 affects the maintenance of dopaminergic neurons in *Drosophila*, EMBO J. 27 (2008) 2432–2443.
[17] M. Jaleel, R.J. Nichols, M. Deak, D.G. Campbell, F. Gillardon, A. Knebel, D.R. Alessi, LRRK2 phosphorylates moesin at threonine-558: characterization of how Parkinson's disease mutants affect kinase activity, Biochem. J. 405 (2007) 307–317.
[18] V.S. Anand, L.J. Reichling, K. Lipinski, W. Stochaj, W. Duan, K. Kelleher, P. Pungaliya, E.L. Brown, P.H. Reinhart, R. Somberg, W.D. Hirst, S.M. Riddle, P.B. Steven, Investigation of leucine-rich repeat kinase 2: enzymological properties and novel assays, FEBS J. 276 (2009) 466–478.
[19] E. Ohta, Y. Katayama, F. Kawakami, M. Yamamoto, K. Tajima, T. Maekawa, N. Iida, S. Hattori, F. Obata, I2020T leucine-rich repeat kinase 2, the causative mutant molecule of familial Parkinson's disease, has a higher intracellular degradation rate than the wild-type molecule, Biochem. Biophys. Res. Commun. 390 (2009) 710–715.
[20] C. Mytilineou, K.S. McNaught, P. Shashidharan, J. Yabut, R.J. Baptiste, A. Parnandi, C.W. Olanow, Inhibition of proteasome activity sensitizes dopamine neurons to protein alterations and oxidative stress, Neural Transm. 111 (2004) 1237–1251.

[21] W.X. Ding, H.M. Ni, X. Chen, J. Yu, L. Zhang, X.M. Yin, A coordinated action of Bax, PUMA, and p53 promotes MG132-induced mitochondria activation and apoptosis in colon cancer cells, Mol. Cancer Ther. 6 (2007) 1062–1069.
[22] B.C. Park, S.H. Park, S.H. Paek, S.Y. Park, M.K. Kwak, H.G. Choi, C.S. Yong, B.K. Yoo, J.A. Kim, Chloroquine-induced nitric oxide increase and cell death is dependent on cellular GSH depletion in A172 human glioblastoma cells, Toxicol. Lett. 178 (2008) 52–60.
[23] E. Biasini, L. Fioriti, I. Ceglia, R. Invernizzi, A. Bertoli, R. Chiesa, G. Forloni, Proteasome inhibition and aggregation in Parkinson's disease: a comparative study in untransfected and transfected cells, J. Neurochem. 88 (2004) 545–553.
[24] L. Fioriti, S. Dossena, L.R. Stewart, R.S. Stewart, D.A. Harris, G. Forloni, R. Chiesa, Cytosolic prion protein (PrP) is not toxic in N2a cells and primary neurons expressing pathogenic PrP mutations, J. Biol. Chem. 280 (2005) 11320–11328.
[25] J. Dunys, T. Kawarai, S. Wilk, P. St. George-Hyslop, C. Alves da Costa, F. Checler, Catabolism of endogenous and overexpressed APH1a and PEN2: evidence for artifactual involvement of the proteasome in the degradation of overexpressed proteins, Biochem. J. 394 (2006) 501–509.
[26] W.W. Smith, Z. Pei, H. Jiang, D.J. Moore, Y. Liang, A.B. West, V.L. Dawson, T.M. Dawson, C.A. Ross, Leucine-rich repeat kinase 2 (LRRK2) interacts with parkin and mutant LRRK2 induces neuronal degeneration, Proc. Natl. Acad. Sci. USA 102 (2005) 18676–18681.
[27] C. Iaccarino, C. Crosio, C. Vitale, G. Sanna, M.T. Carri, P. Barone, Apoptotic mechanisms in mutant LRRK2-mediated cell death, Hum. Mol. Genet. 16 (2007) 1319–1326.
[28] A.K. Liou, R.K. Leak, L. Li, M.J. Zigmond, Wild-type LRRK2 but not its mutant attenuates stress-induced cell death via ERK pathway, Neurobiol. Dis. 32 (2008) 116–124.
[29] D. Wang, B. Tang, G. Zhao, Q. Pan, K. Xia, R. Bodmer, Z. Zhang, Dispensable role of *Drosophila* ortholog of LRRK2 kinase activity in survival of dopaminergic neurons, Mol. Neurodegener. 3 (2008) 3.
[30] M. Baker, I.R. Mackenzie, S.M. Pickering-Brown, J. Gass, R. Rademakers, C. Lindholm, J. Snowden, J. Adamson, A.D. Sadovnick, S. Rollinson, A. Cannon, E. Dwosh, D. Neary, S. Melquist, A. Richardson, D. Dickson, Z. Berger, J. Eriksen, T. Robinson, C. Zehr, C.A. Dickey, R. Crook, E. McGowan, D. Mann, B. Boeve, H. Feldman, M. Hutton, Mutations in progranulin cause tau-negative frontotemporal dementia linked to chromosome 17, Nature 442 (2006) 916–919.
[31] Z.B. Andrews, H. Zhao, T. Frugier, R. Meguro, D.R. Grattan, K. Koishi, I.S. McLennan, Transforming growth factor beta2 haploinsufficient mice develop age-related nigrostriatal dopamine deficits, Neurobiol. Dis. 21 (2006) 568–575.
[32] O. von Bohlen und Halbach, L. Minichiello, K. Unsicker, Haploinsufficiency for trkB and trkC receptors induces cell loss and accumulation of alpha-synuclein in the substantia nigra, FASEB J. 19 (2005) 1740–1742.
[33] M.K. Wetzel, S. Naska, C.L. Laliberté, V.V. Rymar, M. Fujitani, J.A. Biernaskie, C.J. Cole, J.P. Lerch, S. Spring, S.H. Wang, P.W. Frankland, R.M. Henkelman, S.A. Josselyn, A.F. Sadikot, F.D. Miller, D.R. Kaplan, p73 regulates neurodegeneration and phospho-tau accumulation during aging and Alzheimer's disease, Neuron 59 (2008) 708–721.
[34] E. Greggio, I. Zambrano, A. Kaganovich, A. Beilina, J.M. Taymans, V. Daniëls, P. Lewis, S. Jain, J. Ding, A. Syed, K.J. Thomas, V. Baekelandt, M.R. Cookson, The Parkinson disease-associated leucine-rich repeat kinase 2 (LRRK2) is a dimer that undergoes intramolecular autophosphorylation, J. Biol. Chem. 283 (2008) 16906–16914.
[35] M. Hirano, T. Yanagihara, S. Ueno, Dominant negative effect of GTP cyclohydrolase I mutations in dopa-responsive hereditary progressive dystonia, Ann. Neurol. 44 (1998) 365–371.
[36] W.L. Hwu, Y.W. Chiou, S.Y. Lai, Y.M. Lee, Dopa-responsive dystonia is induced by a dominant-negative mechanism, Ann. Neurol. 48 (2000) 609–613.
[37] K. Nocka, J.C. Tan, T.Y. Chu, P. Ray, P. Traktman, P. Besmer, Molecular bases of dominant negative and loss of function mutations at the murine c-kit/white spotting locus: W37, Wv, W41 and W, EMBO J. 9 (1990) 1805–1813.
[38] L.B. Giebel, R.A. Spritz, Mutation of the KIT (mast/stem cell growth factor receptor) protooncogene in human piebaldism, Proc. Natl. Acad. Sci. USA 88 (1991) 8696–8699.

Biochemical and Biophysical Research Communications 392 (2010) 431–435

Contents lists available at ScienceDirect

Biochemical and Biophysical Research Communications

journal homepage: www.elsevier.com/locate/ybbrc

Age-dependent and cell-population-restricted LRRK2 expression in normal mouse spleen

Tatsunori Maekawa, Makoto Kubo, Ikue Yokoyama, Etsuro Ohta, Fumiya Obata *

Division of Clinical Immunology, Graduate School of Medical Sciences, Kitasato University, 1-15-1 Kitasato, Sagamihara, Kanagawa 228-8555, Japan

ARTICLE INFO

Article history:
Received 9 January 2010
Available online 15 January 2010

Keywords:
LRRK2
Mouse spleen
B lymphocytes
Age-related expression
Parkinson's disease

ABSTRACT

Leucine-rich repeat kinase 2 (LRRK2) is the causal molecule of familial Parkinson's disease (PD), but its true physiological function remains unknown. In the normal mouse, LRRK2 is expressed in kidney, spleen, and lung at much higher levels than in brain, suggesting that LRRK2 may play an important role in these organs. Analysis of age-related changes in LRRK2 expression demonstrated that expression in kidney, lung, and various brain regions was constant throughout adult life. On the other hand, expression of both LRRK2 mRNA and protein decreased markedly in spleen in an age-dependent manner. Analysis of purified spleen cells indicated that B lymphocytes were the major population expressing LRRK2, and that T lymphocytes showed no expression. Consistently, the B lymphocyte surface marker CD19 exhibited an age-dependent decrease of mRNA expression in spleen. These results suggest a possibly novel function of LRRK2 in the immune system, especially in B lymphocytes.

Introduction

Leucine-rich repeat kinase 2 (LRRK2) is the causal molecule of autosomal-dominant familial Parkinson's disease (PD), PARK8, which was originally defined in a study of a large Japanese PD family, the Sagamihara family [1–4]. LRRK2 is a large complex protein with an approximate molecular mass of 260 kDa and contains several domains including the LRR (leucine-rich repeat), ROC (Ras of complex), COR (C-terminal ROC), RIP (receptor interacting protein) kinase, and WD40 domains [3–5]. Although the kinase activity toward candidate substrate molecules as well as regulation of the activity by the ROC domain have been studied extensively, the true physiological role of LRRK2 or the mechanism of neurodegeneration resulting from its mutation remains undisclosed.

Analyses of LRRK2 mRNA expression in human, mouse, and rat brain have demonstrated that LRRK2 is expressed in various regions including the substantia nigra, putamen, striatum, amygdala, hippocampus, cortex, and cerebellum [3,4,6–12]. In other organs such as kidney, lung, spleen, and lymph node, expression of LRRK2 mRNA has been reported to be far higher than in brain [6,13,14]. A similar tissue distribution has been reported for LRRK2 protein expression [11,12,15–18]. In contrast to mRNA analysis that uses nucleotide probes and primers specific to the LRRK2 sequence, however, the results of LRRK2 protein expression studies using commercial polyclonal anti-LRRK2 antibodies require careful interpretation because some of the antibodies have been reported to react with proteins around 260 kDa in size other than LRRK2 [13]. With regard to age-related change, LRRK2 mRNA expression in mouse brain, lung, heart, and liver has been reported to increase from embryonic day 11 to birth [13]. After birth, LRRK2 protein in mouse brain has been shown to increase until postnatal day 60 [18]. However, no later adulthood age-related changes in the expression of mouse LRRK2 mRNA or protein have been analyzed in either the brain or other organs, although rat striatum LRRK2 mRNA has been reported to increase until postnatal day 29, remaining constant thereafter until 24 months of age [6].

In the present study, we analyzed the organ/tissue distribution and age-related changes in the expression of mouse LRRK2 at both the mRNA and protein levels, using in the latter case an antibody of validated specificity. We found that LRRK2 was expressed in kidney, lung, and spleen at a level much higher than in any region of the brain. Levels of LRRK2 expression in brain and lung did not change during adulthood. By contrast, in spleen, a marked and age-dependent decrease of LRRK2 expression was found. This finding was explained by an age-dependent decrease of B-lymphocytes, the major LRRK2-expressing cell population, in the spleen.

Materials and methods

Animals. C57BL/6J (B6) mice aged 6–110 weeks were housed in a light- and temperature-controlled room with water and food ad libitum. Organs were removed after euthanasia with carbon dioxide. All procedures had been approved by the Animal Experimentation and Ethics Committee of Kitasato University.

* Corresponding author. Fax: +81 42 778 8075.
E-mail address: obata@ahs.kitasato-u.ac.jp (F. Obata).

0006-291X/$ - see front matter © 2010 Elsevier Inc. All rights reserved.
doi:10.1016/j.bbrc.2010.01.041

Reverse transcription-polymerase chain reaction (RT-PCR). Organs were homogenized in TRIzol Reagent (Invitrogen) and total RNA was isolated in accordance with the manufacturer's instructions. cDNA synthesis was performed by a ThermoScript RT-PCR System (Invitrogen). Quantitative (real-time) PCR was performed using SYBR Green PCR Master Mix and a 7500 Real Time PCR System (Applied Biosystems). PCR primers used were as follows: mouse *LRRK2* forward 5′-TCTGGCTGGAACCCTGCTAT-3′ and reverse 5′- AACTGGC CATCTTCATCTCC-3′, mouse *CD19* forward 5′-AGCGAATGACTGACCC CGCC-3′ and reverse 5′- CCAGGCCCATGCTCAGCGTT-3′, mouse *glyceraldehyde-3-phosphate dehydrogenase (GAPDH)* forward 5′- GAGGC CGGTGCTGAGTATGTCGTG-3′ and reverse 5′- TCGGCAGAAGGGGCG GAGAT-3′. The threshold cycle (C_t) value of *LRRK2* was normalized by the C_t value of the *GAPDH* gene.

Western blotting. Tissues were homogenized in digitonin buffer [1% digitonin, Tris-buffered saline (pH 7.6), 1 mM phenylmethylsulfonyl fluoride, and a protease inhibitor cocktail tablet (Roche)], and rotated at 4 °C for 1 h. Tissue lysates obtained by centrifugation were subjected to sodium dodecyl sulfate polyacrylamide gel electrophoresis (SDS–PAGE) using a 5–20% gradient e-PAGEL (ATTO), and blotted onto polyvinylidene fluoride membranes. The membranes were blocked in 2% skim milk or 2% ECL Advance Blocking Agent (GE Healthcare) in phosphate-buffered saline (PBS)-Tween 20 overnight at 4 °C. The membranes were probed with a rabbit polyclonal antibody against LRRK2 (AT106, Alexis) for 45 min at room temperature. After incubation with horseradish peroxidase (HRP)-labeled donkey anti-rabbit IgG (BioLegend) secondary antibody, bands were visualized using an ECL or ECL Advance Western Blotting Detection Kit (GE Healthcare). HRP-labeled monoclonal antibody against beta actin (Abcam) was used as a control.

Purification of spleen cell subpopulations. Spleens were cut into small pieces, filtered through nylon mesh to disperse single cells, and treated with hypotonic solution to lyse erythrocytes. T lymphocytes, B lymphocytes, and macrophages were separated using magnetic beads conjugated with antibodies against the cell surface markers, CD3, CD19, and CD11b, respectively, and LS Column Adaptor (Miltenyi Biotec). Cell population purity was confirmed by flow cytometry to be 92.5% for CD3, 96.8% for CD19, and 88.5% for CD11b.

Results

Expression of LRRK2 mRNA in adult mouse organs

To examine the expression level of mouse LRRK2 mRNA, quantitative PCR of various organs from C57BL/6J mice aged 20, 50, and 98 weeks was performed. This revealed that expression of LRRK2 mRNA in kidney, spleen, lung, and testis was high in mice at these ages, whereas expression in each of the brain regions examined (cortex, cerebellum, midbrain, medulla, and olfactory bulb), as well as in liver and heart, was low at the same ages (Fig. 1). Notably, the level of LRRK2 mRNA in the spleen of mice aged 98 weeks was much lower than that at 20 and 50 weeks, suggesting an age-related change in the mRNA level.

Relationship between expression of LRRK2 mRNA and aging

To further investigate the age-dependency of LRRK2 mRNA expression, spleen, lung, cortex, midbrain, and cerebellum of mice aged 6, 18, 34, 70, and 110 weeks were analyzed. In accordance with the results shown in Fig. 1, quantitative PCR analysis of the spleen indicated that expression of LRRK2 mRNA decreased markedly in an age-dependent manner (Fig. 2). The splenic level of LRRK2 mRNA at 70 and 110 weeks was about one fifth and one eighth of that at 6 weeks, respectively. On the other hand, the levels of LRRK2 mRNA in lung, cortex, midbrain, and cerebellum remained almost constant as aging progressed.

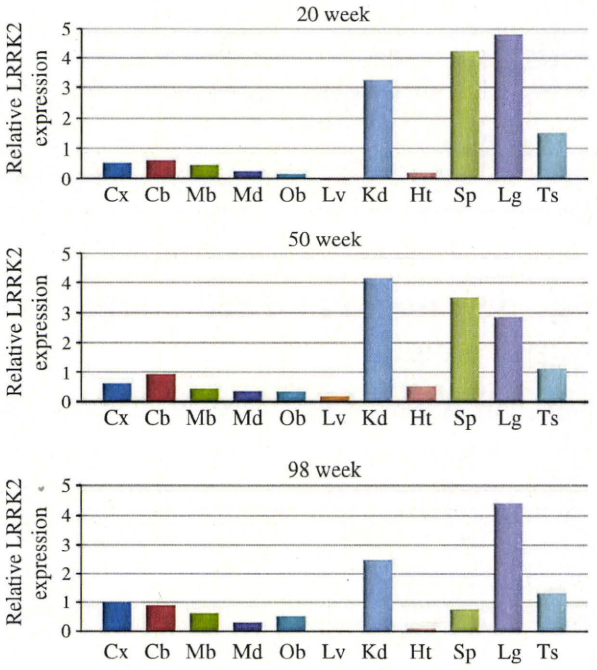

Fig. 1. Expression of LRRK2 mRNA in various organs of adult mouse. RNA was isolated from various organs of C57BL/6J mice aged 20, 50, and 98 weeks and subjected to quantitative PCR. Relative expression of *LRRK2* normalized by *GAPDH* is shown.

Expression of LRRK2 protein in adult mouse organs

AT106 is one of two commercial polyclonal antibodies that have been proved to recognize the endogenous mouse LRRK2 molecule by using knockout mice as a negative control [13]. As reported, Western analysis using this antibody identified LRRK2 proteins of about 260 kDa just below the nonspecific band (Supplementary Fig. 1A). Western analysis of lysates of various tissues from mice aged 50 weeks revealed that the levels of LRRK2 protein in these organs were consistent with the corresponding mRNA levels in each organ at the same age, as shown in Fig. 1, i.e., high in kidney, spleen, lung, and testis, but low in various brain regions (cortex, cerebellum, midbrain, medulla, and olfactory bulb), liver, and heart (Supplementary Fig. 1B).

Age-related changes in the splenic level of LRRK2 protein

To investigate age-related changes in the expression of LRRK2 protein in the spleen, tissue lysates of spleen and lung from mice aged 6, 18, 34, 70, and 110 weeks were subjected to Western analysis using AT106 antibody. Consistent with the results of mRNA analysis, the splenic level of LRRK2 protein decreased markedly with aging (Fig. 3). The level of LRRK2 protein at 70 and 110 weeks was about one third and one twelfth of that at 6 weeks, respectively. Thus, LRRK2 protein expression in the spleen was found to exhibit an age-dependent decrease like that of the mRNA.

LRRK2 expression in spleen cell subpopulations

Because the spleen contains various populations of immune cells, we next purified each population with magnetic bead-conju-